Argonaute2 complexes carry a population of circulating microRNAs independent of vesicles in human plasma

Jason D. Arroyo[a], John R. Chevillet[a], Evan M. Kroh[a], Ingrid K. Ruf[a], Colin C. Pritchard[b], Donald F. Gibson[b], Patrick S. Mitchell[a,1], Christopher F. Bennett[a,c], Era L. Pogosova-Agadjanyan[d], Derek L. Stirewalt[d], Jonathan F. Tait[b], and Muneesh Tewari[a,d,e,2]

[a]Division of Human Biology, Fred Hutchinson Cancer Research Center, Seattle, WA 98109-1024; [b]Department of Laboratory Medicine, University of Washington Medical Center, Seattle, WA 98195-7110; [c]Molecular and Cellular Biology Program, University of Washington, Seattle, WA 98195; and Divisions of [d]Clinical Research and [e]Public Health Sciences, Fred Hutchinson Cancer Research Center, Seattle, WA 98109-1024

Edited* by Robert N. Eisenman, Fred Hutchinson Cancer Research Center, Seattle, WA, and approved February 9, 2011 (received for review December 21, 2010)

MicroRNAs (miRNAs) circulate in the bloodstream in a highly stable, extracellular form and are being developed as blood-based biomarkers for cancer and other diseases. However, the mechanism underlying their remarkable stability in the RNase-rich environment of blood is not well understood. The current model in the literature posits that circulating miRNAs are protected by encapsulation in membrane-bound vesicles such as exosomes, but this has not been systematically studied. We used differential centrifugation and size-exclusion chromatography as orthogonal approaches to characterize circulating miRNA complexes in human plasma and serum. We found, surprisingly, that the majority of circulating miRNAs cofractionated with protein complexes rather than with vesicles. miRNAs were also sensitive to protease treatment of plasma, indicating that protein complexes protect circulating miRNAs from plasma RNases. Further characterization revealed that Argonaute2 (Ago2), the key effector protein of miRNA-mediated silencing, was present in human plasma and eluted with plasma miRNAs in size-exclusion chromatography. Furthermore, immunoprecipitation of Ago2 from plasma readily recovered non–vesicle-associated plasma miRNAs. The majority of miRNAs studied copurified with the Ago2 ribonucleoprotein complex, but a minority of specific miRNAs associated predominantly with vesicles. Our results reveal two populations of circulating miRNAs and suggest that circulating Ago2 complexes are a mechanism responsible for the stability of plasma miRNAs. Our study has important implications for the development of biomarker approaches based on capture and analysis of circulating miRNAs. In addition, identification of extracellular Ago2–miRNA complexes in plasma raises the possibility that cells release a functional miRNA-induced silencing complex into the circulation.

microvesicles | diagnostic

MicroRNAs (miRNAs) are a class of approximately 22 nucleotide noncoding RNAs that mediate posttranscriptional gene regulation by binding to and repressing specific messenger RNA targets. We and others previously demonstrated that miRNAs are present in the human circulation in a cell-free form and that altered plasma and serum miRNA profiles are observed in cancer and other diseases (1–9). This, along with the finding that miRNAs are remarkably stable in plasma despite high circulating RNase activity (1), suggests that miRNAs may be developed into a powerful new class of blood-based biomarkers.

The mechanism underlying the unexpected stability of cell-free miRNAs in the RNase-rich environment of blood has not been systematically investigated, although it has important implications for miRNA biomarker development and for potential biological functions of circulating miRNAs (10). Currently, the dominant model for circulating miRNA stability is that miRNAs are released from cells in membrane-bound vesicles, which protect them from blood RNase activity. Vesicles proposed as carriers of circulating miRNAs include exosomes, which are 50- to 90-nm vesicles arising from multivesicular bodies and released by exocytosis (11), as well as larger membrane-bound particles including microvesicles that range in size to as large as 1 μm (12, 13). This model is supported by the observation that cells growing in culture release exosomes that are associated with miRNA (6, 14–16) and by the detection of miRNAs associated with exosomes and microvesicles isolated from plasma and serum (7, 13, 17, 18). However, a systematic investigation of the physiologic state of circulating miRNAs in plasma has not yet been reported to our knowledge, and it is not known if vesicle encapsulation is the only mechanism for circulating miRNA stability or if other potentially more predominant mechanisms exist.

We report here a systematic investigation of the physical state of miRNAs in plasma and serum, which provides insight into mechanisms accounting for circulating miRNA stability. We show that vesicle-encapsulated miRNAs represent only a minor portion of circulating miRNAs. In particular, we report that a significant portion of circulating miRNA is associated with Argonaute2 (Ago2), the effector component of the miRNA-induced silencing complex that directly binds miRNAs and mediates messenger RNA repression in cells (19–22). These results substantially revise the current understanding of the physiological state and basis for stability of circulating miRNAs, and we discuss the implications for future studies of miRNA biomarkers and extracellular miRNA function.

Results

Circulating miRNAs Are Not Intrinsically Resistant to Plasma RNases. In taking a systematic approach to identify mechanisms that protect circulating miRNAs, the first hypothesis we examined was that circulating miRNAs are intrinsically resistant to RNase activity in blood. If plasma-derived miRNAs are intrinsically resistant, the addition of purified plasma miRNA to fresh plasma samples is expected to yield an increase in miRNA abundance. However, we observed that purified plasma miRNA was rapidly degraded when incubated with plasma, whereas previous inhibition of plasma RNase activity blocked this degradation

Author contributions: J.D.A., J.R.C., C.C.P., P.S.M., J.F.T., and M.T. designed research; J.D.A., J.R.C., E.M.K., I.K.R., C.C.P., D.F.G., P.S.M., C.F.B., and J.F.T. performed research; E.L.P.-A. and D.L.S. contributed new reagents/analytic tools; J.D.A., J.R.C., E.M.K., I.K.R., P.S.M., J.F.T., and M.T. analyzed data; and J.D.A. and M.T. wrote the paper.

The authors declare no conflict of interest.

*This Direct Submission article had a prearranged editor.

Freely available online through the PNAS open access option.

[1]Present address: Division of Basic Sciences, Fred Hutchinson Cancer Research Center, Seattle, WA 98109-1024; and Molecular and Cellular Biology Program, University of Washington, Seattle, WA 98195.

[2]To whom correspondence should be addressed. E-mail: mtewari@fhcrc.org.

This article contains supporting information online at www.pnas.org/lookup/suppl/doi:10.1073/pnas.1019055108/-/DCSupplemental.

(Fig. S1). Therefore, we concluded that circulating miRNAs are not intrinsically resistant to endogenous RNase activity.

Circulating miRNAs Are Not Restricted to Vesicles. We next tested the hypothesis that circulating miRNAs are primarily encapsulated in membrane-bound vesicles. Studies that used differential ultracentrifugation to purify vesicles have proposed that microvesicles and exosomes serve as the carriers of circulating miRNAs and protect them from RNase activity (6, 7, 13, 17). However, a quantitative analysis of the proportion of circulating miRNAs that are in fact vesicle-associated has not been reported to our knowledge.

To determine the extent to which circulating miRNAs are associated with microvesicles and/or exosomes, we used differential ultracentrifugation to purify circulating vesicles from cell-free, platelet-poor plasma prepared from three healthy individuals (Fig. S2*A*). Platelet-poor plasma was chosen to minimize residual platelets that occur with standard plasma protocols. Platelet-poor plasma was prepared by centrifugation of anticoagulated blood twice, which reduces platelet levels more than 100 fold compared with normal whole blood (23) to 1,000 to 2,000 platelets/μL, as measured by automated complete blood cell counts. Platelet-poor plasma was processed within 1 h of blood draw and used fresh (never frozen) for ultracentrifugation within 4 h of draw. We confirmed recovery of vesicles consistent in size and morphology with exosomes and microvesicles by EM (Fig. 1*A*). By using quantitative RT-PCR (qRT-PCR), we assayed the vesicle pellets and the vesicle-poor supernatants for three well characterized circulating miRNAs: miR-16, miR-92a, and let-7a (1, 8, 24). We determined miRNA copies by absolute quantification and normalized between samples using synthetic *Caenorhabditis elegans* miRNA oligonucleotides that were spiked into each sample after RNase inactivation (1, 25). We observed that approximately 95% of the circulating miR-16 and miR-92a did not pellet with vesicles (Fig. 1*B*). In contrast, we detected 40% to 75% of circulating let-7a in the vesicle pellet. Thus, the results from differential ultracentrifugation suggested at least two populations of circulating miRNAs exist in plasma: those that are strongly associated with the vesicle-rich pellet and those that are not.

Although ultracentrifugation successfully recovered vesicles from plasma, it is possible that miRNA remained in the supernatant as a result of incomplete vesicle recovery or vesicle rupture under the high force conditions of ultracentrifugation. To address these caveats, we applied size-exclusion chromatography as an orthogonal approach to characterize circulating miRNAs (Fig. S2*B*). We fractionated miRNA-containing particles under gentle conditions with Sephacryl S-500 resin. Based on vesicle and protein standards, we determined that our column resolves particles from approximately 1 to 120 nm in diameter, with particles 120 nm and larger eluting near fraction 8 and particles 1 nm or smaller eluting near fraction 20 (Fig. 2*D* and Fig. S3). Plasma was prepared freshly from three healthy donors within 1 h of blood draw, and the never-frozen plasma samples were applied to the column within 4 h of blood draw. The copies of miR-16, miR-92a, and let-7a were quantified in each fraction by qRT-PCR and normalized to spiked-in synthetic *C. elegans* miRNAs to correct for fraction-to-fraction technical differences in miRNA extraction efficiency. Protein abundance of each fraction was measured by absorbance at 280 nm.

We observed that two populations of circulating miRNAs separated based on the size of their associated particles. In all three plasma samples, miR-16 and miR-92a cofractionated with the relatively small protein components of plasma in fractions 15 to 21 (Fig. 2 *A*–*C*). In contrast, the majority of let-7a eluted earlier in fractions 8 to 10 that are expected to contain large complexes and vesicles, and only low levels of let-7a were detectable in the late fractions. We also analyzed serum prepared in parallel from the same donors (*SI Results*). We observed similar serum miRNA distributions, although miR-16 and miR-92a were detected in early serum fractions (Fig. S4 *A*–*C*). As with our ultracentrifugation experiment, the results for miR-16 and miR-92a indicate that these miRNAs are not vesicle-associated. Instead, our data suggest that specific circulating miRNAs exist within a ribonucleoprotein complex.

To examine whether the early-eluting miRNA population was likely to represent a size range corresponding to vesicles, we determined the elution profile of synthetic lipid vesicles with a nominal average diameter of 100 nm (Fig. 2*D*). We also analyzed the elution of BSA and tyrosine as protein and small-molecule standards, respectively. When we compared the elution of the standards versus the distribution of miRNAs in plasma, we observed that let-7a eluted in fractions consistent with an association with vesicles (fractions 8–10). In contrast, our vesicle standard was not present in the late fractions that contain the majority of miR-16 and miR-92a. These results are consistent with the conclusion that there are vesicle-associated and non–vesicle-associated populations of circulating miRNAs. Our data strongly support the hypothesis that at least two circulating miRNAs—miR-16 and miR-92a—are predominantly contained within a ribonucleoprotein complex in plasma and are not significantly associated with exosomes.

A Protease-Sensitive Complex Specifically Stabilizes Circulating miRNAs Present in Late Chromatography Fractions. Because our fractionation analysis suggested that miR-16 and miR-92a were in a ribonucleoprotein complex, we examined whether such a complex was responsible for the stability of these miRNAs in plasma. We hypothesized that, if a protein complex stabilized circulating miRNAs, proteolytic digestion of that complex would release the miRNAs and render them sensitive to degradation by plasma RNase activity. However, miRNAs stabilized through a vesicle mechanism would not be expected to show sensitivity to proteolysis. We incubated untreated plasma and plasma treated with DNase/RNase-free proteinase K at 55 °C, as these were the conditions required for proteinase K treatment. We observed that miR-16 and miR-92a were rapidly destabilized and degraded in the presence of proteinase K but were stable in the untreated control (Fig. 3 *A* and *B*). The early-eluting miRNA let-7a was not sensitive to proteinase K treatment, exhibiting no substantial difference between untreated and treated samples (Fig. 3*C*). Interestingly, let-7a showed a slow time-dependent decline in the untreated and treated plasma samples, which we speculate might have resulted from loss of vesicle integrity

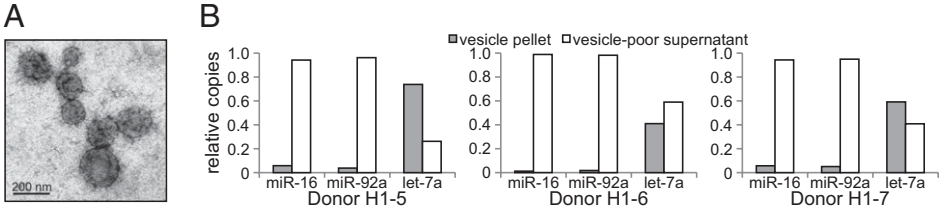

Fig. 1. Circulating miRNAs are not restricted to vesicles. (*A*) Circulating vesicles were purified from plasma by differential ultracentrifugation. Recovery of vesicles consistent in size and morphology with exosomes and microvesicles was confirmed by EM. A representative micrograph is shown. (*B*) The plasma vesicle pellet (gray bars) and vesicle-poor supernatant (white bars) from the indicated donors were assayed for miR-16, miR-92a, and let-7a by using TaqMan qRT-PCR. For each miRNA, a standard curve of the corresponding synthetic oligonucleotide enabled absolute quantification of miRNA copies. Bars represent relative copies of miRNA recovered from the pellet and supernatant.

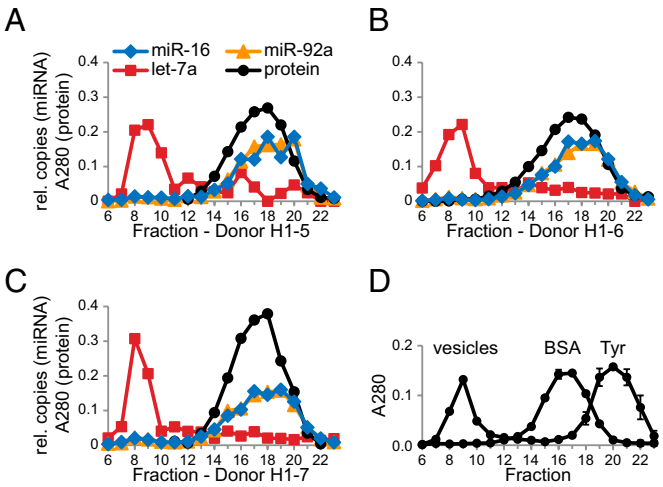

Fig. 2. Two populations of circulating miRNAs are identified by size-exclusion chromatography. (*A*–*C*) Plasma samples from the indicated donors were fractionated on a Sephacryl S-500 column. Fractions were assayed for miR-16 (blue diamond), miR-92a (orange triangle), and let-7a (red square) by using absolute quantification by TaqMan qRT-PCR. Protein abundance was determined by absorbance at 280 nm (A280; black circle). For miRNAs, the *y*-axis values indicate relative copies of miRNA in each fraction. For protein, the same *y*-axis values indicate A280 reading. (*D*) Elution profiles of vesicles (100 nm mean diameter), BSA, and tyrosine standards were determined by A280. Points represent the mean ± SD of duplicate independent analyses.

caused by incubation at 55 °C. The results demonstrate that a protease-sensitive complex specifically stabilizes late-eluting but not early-eluting circulating miRNAs and further support the model of a ribonucleoprotein complex that is responsible for the stability of nonvesicular circulating miRNAs.

Majority of Circulating miRNAs Have a Size-Exclusion Chromatography Profile Consistent with Non–Vesicle-Associated Ribonucleoprotein Complexes. Although we detected two populations of circulating miRNAs, our initial experiments focused on only three miRNAs. We therefore sought to determine how other circulating miRNAs distribute into these populations. We used qRT-PCR miRNA profiling arrays to measure the abundance of 375 miRNAs in the plasma and serum fractions from a single donor, H1-7. To increase the amount of RNA that could be used, adjacent pairs of fractions were pooled at the RNA level before the analysis.

miRNA profiling platforms have assay-specific limits of linear quantification, and many circulating miRNAs are present at low levels that may be near or below such limits. To ensure the reliability of our profiling data, we performed dilution analysis of circulating miRNAs purified from unfractionated plasma or serum from the same donor to empirically determine the limits of linear quantification and detection and the PCR efficiency for the 375 miRNAs analyzed. Based on dilution analysis, we removed nonlinear assays from further analysis and performed nonspecific filtering to remove unreliable C_T values beyond the assay-specific detection limits. We reliably detected 128 and 136 miRNAs in unfractionated plasma and serum, respectively (Tables S1 and S2), which was comparable to our profiling analysis in a previous study (1). After chromatography was performed and its associated diluting effect occurred, 88 plasma and 66 serum miRNAs were reliably quantifiable in at least one fraction. For these miRNAs, we calculated relative quantification (RQ) across all fraction pools, based on assay-specific PCR efficiency. Hierarchical clustering was performed independently on the plasma and serum profiling datasets (Fig. 4*A* and Fig. S4*D*). This analysis revealed three broad classes of circulating miRNAs: those enriched in large particle fractions 6 to 11, those enriched in small particle fractions 14 to 21, and those distributed between both peaks. Approximately 15% of the detected circulating miRNAs in plasma and serum were enriched in early fractions, consistent with vesicles. However, the majority of circulating miRNAs were detected in the smaller particle fractions. We observed that 66% (plasma) and 68% (serum) of the detectable miRNAs were enriched in late fractions, consistent with a ribonucleoprotein complex, and the remaining miRNAs were present at similar levels in early and late peaks. Moreover, 43% (plasma) and 27% (serum) of the detectable miRNAs were detected in only the late fractions.

To validate the results of our profiling experiment, we compared the profiling data for let-7a, miR-16, and miR-92a (Fig. 4*A* and Fig. S4*D*) with our previous analysis of the same donor by individual qRT-PCR assays (Fig. 2*C* and Fig. S4*C*). Overall, the RQ of these miRNAs determined by miRNA profiling was concordant with the relative copy numbers measured by TaqMan qRT-PCR in plasma and serum fractions. The only exception was let-7a in the plasma profiling, which failed to pass our nonspecific filtering in the qRT-PCR array and was excluded from the plasma profiling analysis. This may be explained by the lower sensitivity of the qRT-PCR array platform (as a result of a smaller RNA input amount per assay) compared with the individual miRNA qRT-PCR assays used in our earlier analysis.

To further confirm the miRNA distributions identified by profiling, we chose three additional miRNAs from the profiling data to validate by individual TaqMan qRT-PCR assays. miRNAs were chosen to represent each class of circulating miRNA defined by clustering: miR-142–3p (early-eluting), miR-122 (late-eluting), and miR-150 (distributed in both peaks). The copy number of these miRNAs was assayed in each fraction from the same profiled donor. Consistent with our profiling results, we observed that miR-142–3p was predominantly localized in early fractions 8 and 9 in plasma and serum (Fig. 4*B*). The TaqMan assay was more sensitive than the profiling platform and also detected a low level of miR-142–3p in later fractions. The distribution of miR-150 and miR-122 as detected by TaqMan also matched the profiling in both plasma and serum, confirming that miR-150 was evenly distributed whereas miR-122 was restricted to the late fractions (Fig. 4 *C* and *D*). We observed similar distributions of these miRNAs in our other two donors, although miR-142–3p dem-

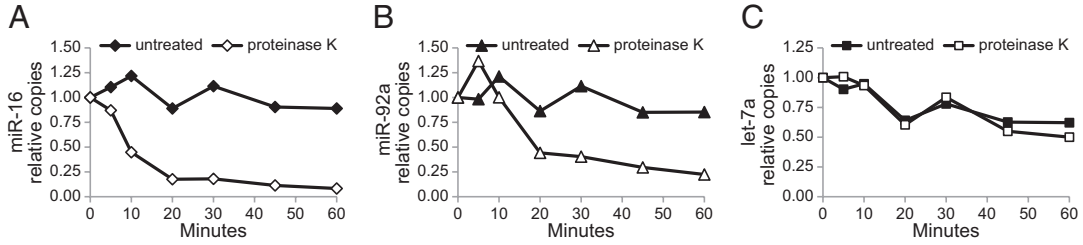

Fig. 3. A protease-sensitive complex protects late-eluting miRNAs from plasma RNase activity. Plasma was untreated (closed symbols) or treated with proteinase K (5 mg/mL; open symbols) at 55 °C. At times indicated, aliquots were removed and assayed for miR-16 (*A*), miR-92a (*B*), and let-7a (*C*) by qRT-PCR. Points represent miRNA copies detected at each time relative to the corresponding 0-min sample.

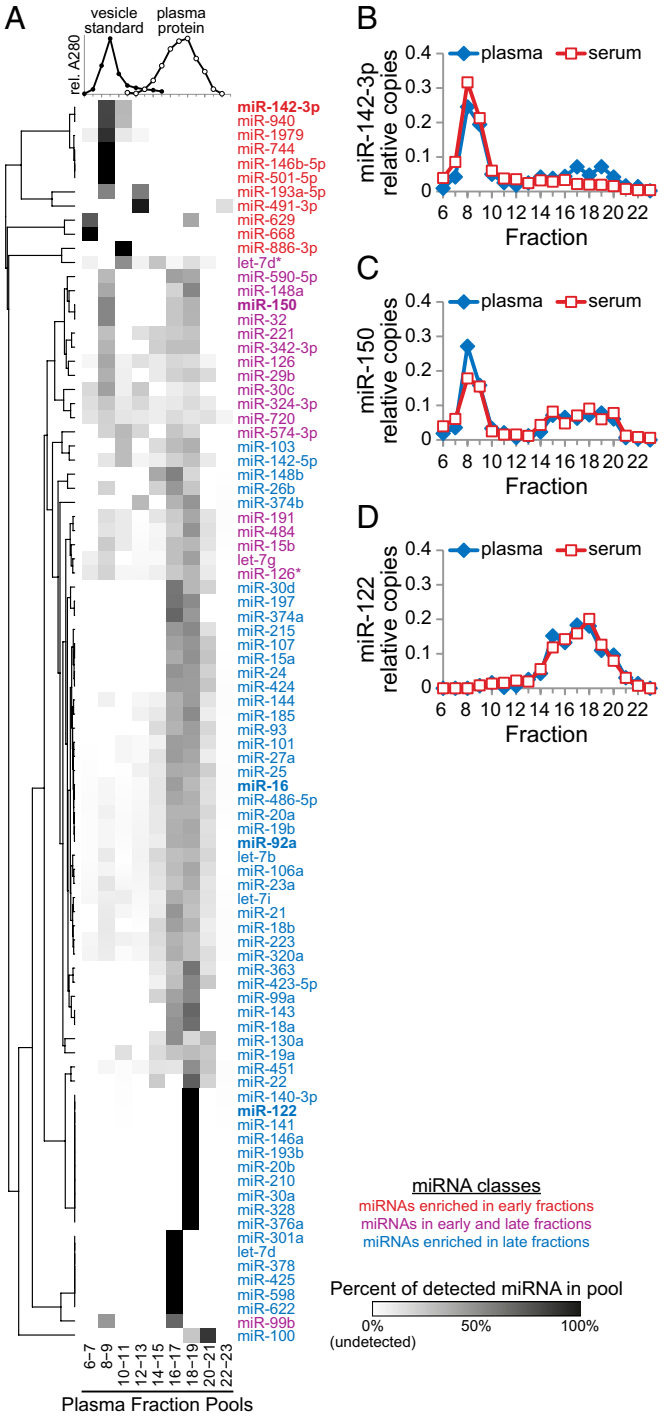

Fig. 4. Circulating miRNAs are predominantly in fractions consistent with ribonucleoprotein complexes. (*A*) RQ of circulating miRNAs profiled in the indicated plasma fraction pools (donor H1-7) is presented as a heat map. Shading represents miRNA level detected in a given fraction pool relative to the total of that miRNA detected across all pools. Above the heat map is a composite of the vesicle standard and corresponding plasma protein elution profile from Fig. 2 (vesicle and protein A280 values are scaled so peaks are the same height). Hierarchical clustering ordered miRNAs as indicated by the dendrogram. Assay names are colored by three classes: early-eluting (red), late-eluting (blue), and eluting in both peaks (purple). Boldface miRNAs were measured by individual TaqMan qRT-PCR assays. Validation of miR-142–3p (*B*), miR-150 (*C*), and miR-122 (*D*) levels in fractions of plasma (blue diamonds) and serum (red squares) from donor H1-7. Points represent the miRNA relative copies in fractions as determined by TaqMan qRT-PCR and absolute quantification.

onstrated individual variability (*SI Results* and Fig. S5). Thus, by using multiple miRNA assays, we demonstrated that the distributions of circulating miRNAs detected by profiling were valid and reproducible within the limits of detection for the platform.

Circulating miRNAs Are Associated with Circulating Ago2 Complexes. In mammalian cells, mature miRNAs are loaded into Argonaute (Ago) complexes that mediate messenger RNA silencing activity (26). However, cell-free Ago complexes in the circulation have not been previously reported. Based on our observation that the majority of circulating miRNAs fractionate in a manner consistent with a ribonucleoprotein complex, we hypothesized that these miRNAs are present within circulating Ago complexes. Four Ago proteins have been identified in mammals, of which Ago2 is the best characterized. To determine if Ago proteins are present in plasma, we performed immunoprecipitation followed by immunoblotting with antibodies against each of the four known human Ago proteins. Detergent was not added during immunoprecipitation to avoid potential lysis of plasma vesicles. Although we were unable to detect Ago1, Ago3, or Ago4 with the available antibodies, we observed Ago2 in human plasma (Fig. 5*A*). Without immunoprecipitation, Ago2 levels in plasma were below the limit of detection by immunoblotting. The absence of Ago2 in negative control IgG immunoprecipitates demonstrated that Ago2 was specifically precipitated from plasma.

To determine whether circulating miRNAs are associated with Ago2, the Ago2 and control IgG immunoprecipitates were assayed for miR-16, miR-92a, and let-7a. Compared with the abundance of these miRNAs in total plasma, 17% to 26% of the miR-16 and 11% to 22% of the miR-92a was present in the Ago2 immunoprecipitates, depending on the donor (Fig. 5*B*, *Upper*). This recovery may underestimate the Ago2-associated miRNA because Ago2 immunoprecipitation efficiency is likely less than 100%. Although we were unable to determine the Ago2 immunoprecipitation efficiency from plasma as a result of the technical limitations of direct Ago2 immunoblotting of plasma input, we observed that the efficiency from cell lysates using the same antibody is, at most, 60% (Fig. S6). On average, the levels of miR-16 and miR-92a detected in Ago2 immunoprecipitates were 55- and 30-fold greater, respectively, than in negative control IgG immunoprecipitates, indicating that these miRNAs were specifically associated with Ago2-containing complexes. In con-

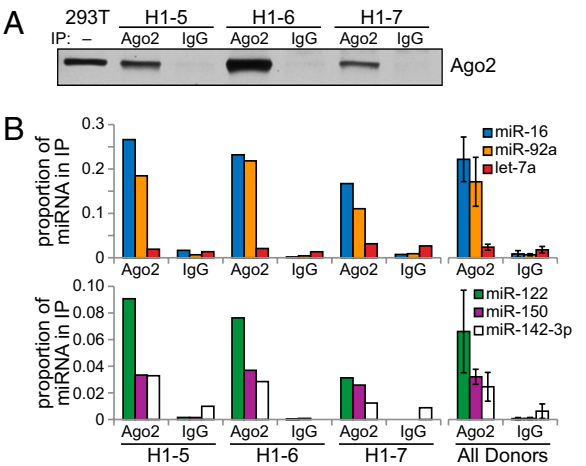

Fig. 5. Cell-free circulating Ago2–miRNA ribonucleoprotein complexes exist in human plasma. (*A*) Ago2 immunoprecipitated from fresh platelet-poor plasma from three healthy donors was detected by immunoblotting. Immunoprecipitation with normal mouse IgG served as a negative control. 293T cell lysate was a positive control for Ago2. (*B*) Immunoprecipitates in *A* were assayed for the indicated miRNAs. Bars represent the proportion of miRNA that was recovered in the immunoprecipitate from the plasma volume used for immunoprecipitation. Bars labeled "All Donors" represent the mean ± SD of the three donors.

trast, both Ago2 and control IgG antibodies precipitated similar, minimal levels of let-7a in each donor, consistent with our hypothesis that early-eluting miRNAs are present within vesicles. We also assayed the immunoprecipitates for the three additional miRNAs identified by profiling (Fig. 5*B*, *Lower*). All three donors showed significant enrichment (>20 fold) of miR-122 and miR-150 in the Ago2 immunoprecipitates versus IgG controls. Donor H1-7, who lacked late-eluting miR-142–3p (Fig. 4*B*), also showed little or no specific coprecipitation of miR-142–3p with Ago2 (Fig. 5*B*). However, donors H1-5 and H1-6 had early and late miR-142–3p (Fig. S5) and subsequently showed specific coprecipitation of miR-142–3p with Ago2 compared with the IgG control (Fig. 5*B*). Overall, each late-eluting miRNA we examined showed specific association with plasma-derived Ago2 complexes, but miRNAs restricted to early fractions were not accessible to Ago2 immunoprecipitation.

To further test our hypothesis that late-eluting circulating miRNAs are associated with Ago2, we determined the elution profile of Ago2 on our column. With the same plasma fractions described previously, we performed Ago2 immunoprecipitation/immunoblotting. Fractions were not frozen before immunoprecipitation and no detergent was used to avoid potential lysis of vesicles present in early fractions. We detected Ago2 in the fractionated plasma of all three donors (Fig. 6*A*, *Lower*). Ago2 was broadly distributed in a single peak across fractions 13 to 21 and was not detected in early fractions. This distribution is consistent with a non–vesicle-associated Ago2 complex in the circulation. We compared the elution profile of Ago2 to the average relative abundance of miR-16, miR-92a, and let-7a previously determined for each fraction and found that Ago2 cofractionated with miR-16 and miR-92a but not let-7a (Fig. 6*A*). Thus, Ago2 cofractionates with late-eluting miRNAs, as expected for a ribonucleoprotein complex, rather than with early-eluting miRNAs that may be associated with vesicles.

To confirm that the Ago2 observed in the plasma fractions was bound to the cofractionating miRNA, we assayed the Ago2 immunoprecipitates of each plasma fraction for miRNA. We consistently detected miR-16, miR-92a, and miR-122, which were all strongly enriched in late fractions, in these Ago2 immunoprecipitates from fractionated human plasma across all donors (Fig. 6*B*). miR-150 and miR-142–3p were also detected but at lower levels, consistent with their presence in early and late fractions. In contrast, very low levels of the early eluting miRNA let-7a were present in Ago2 immunoprecipitates. Notably, Ago2 immunoprecipitation from plasma fractions appeared to more efficiently recover miRNAs compared with the immunoprecipitation from unfractionated plasma described earlier. Combining the Ago2-associated miRNA present across fractions indicated that, on average, 27% of miR-92a, 25% of miR-16 and miR-122, and 16% of miR-150 and miR-142–3p was associated with Ago2 (Fig. 6*C*). Taken together, our results indicate that these circulating miRNAs are present within nonvesicular Ago2 ribonucleoprotein complexes and support these complexes as a mechanism for circulating miRNA stability.

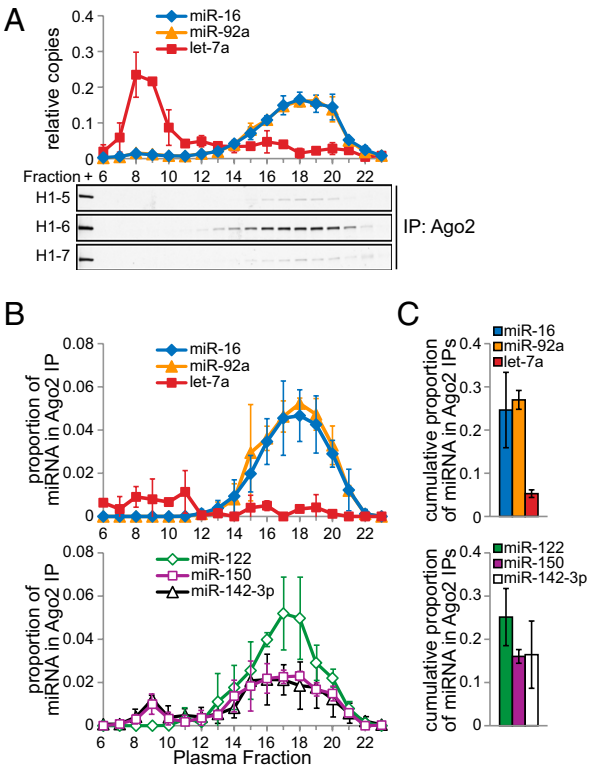

Fig. 6. Late-eluting miRNAs are specifically present within circulating Ago2 ribonucleoprotein complexes. (*A*) Relative copies of miR-16, miR-92a, and let-7a in each plasma fraction shown in Fig. 2 *A*–*C* were averaged (*Upper*). Points represent the mean ± SD of the three donors. Ago2 immunoprecipitated from the same plasma fractions of the indicated donors was detected by immunoblotting (*Lower*). 293T cell lysate (lane marked "+") was a positive control for immunoblotting. Fraction numbers refer to both panels. (*B*) Plasma fraction Ago2 immunoprecipitates in *A* were assayed for the indicated miRNAs. The *y* axes correspond to the proportion of each miRNA recovered in the Ago2 immunoprecipitate of a given fraction relative to the total of that miRNA detected across all plasma fractions for the respective donor. Points represent the mean ± SD from three donors. (*C*) For each donor, the cumulative miRNA detected in Ago2 immunoprecipitates of all plasma fractions relative to the total miRNA detected in all plasma fractions was calculated. Bars represent the mean ± SD for three donors.

Discussion

Recent studies have found that extracellular miRNAs are associated with microvesicles and exosomes, leading to the current model that miRNAs in the circulation are protected from RNases via encapsulation in vesicles. By using a systematic approach to characterize circulating miRNAs, we discovered that there are at least two populations of circulating miRNAs. Although we confirmed some plasma miRNAs to be vesicle-associated, these represented the minority, whereas potentially 90% of miRNAs in the circulation are present in a non–membrane-bound form consistent with a ribonucleoprotein complex. These non–vesicle-associated miRNAs were specifically destabilized by proteinase K digestion of plasma, further supporting protection by a protein complex as a mechanism for their stability in the RNase-rich circulation. We established the existence of such a complex by immunoprecipitation and identified a circulating Ago2–miRNA complex distinct from vesicles. For the miRNAs we studied in depth, every miRNA present in late chromatography fractions was also detected in immunoprecipitated circulating Ago2 ribonucleoprotein complexes. Thus, our study reveals an extracellular localization of Ago2–miRNA complexes in the human circulation and provides a model for the stability of nonvesicular circulating miRNAs.

It is notable that we observed miRNAs that are exclusively associated with vesicles, as well as miRNAs that were exclusively recovered in the ribonucleoprotein complex fractions. Although several interpretations are possible, we hypothesize that vesicle-associated versus Ago2 complex-associated miRNAs originate from different cell types and reflect cell type-specific miRNA expression and/or release mechanisms. For example, the liver-specific miRNA miR-122 (27) was detected only in the protein-associated fractions, suggesting that hepatocytes may release miR-122 through a protein carrier pathway. In contrast, miRNAs that were predominantly vesicle-associated, such as let-7a, might originate from cell types known to generate vesicles, including reticulocytes releasing exosomes during maturation to erythrocytes (28) or platelets shedding microvesicles upon activation (12, 13).

The identification of distinct circulating miRNA populations may impact the development of specific miRNAs as biomarkers. For biomarker miRNAs found to segregate to specific com-

plexes, purification strategies may serve to enrich those miRNAs and increase biomarker sensitivity. Strategies for miRNA biomarker analysis based on exosome purification have already been proposed (6, 7, 18). Our findings would suggest that such strategies may be ineffective for miRNA biomarkers that circulate as nonexosomal Ago2 complexes, and that immunoaffinity enrichment of Ago2 complexes may be an effective strategy for improving sensitivity and miRNA biomarker performance in many cases.

Although miRNAs were consistently detected in Ago2 complexes, we found that a fraction of each assayed miRNA remained in the supernatant following Ago2 immunoprecipitation. Given that immunoprecipitation efficiency from cell lysates was, at most, 60% and could be even lower from plasma, it is conceivable that Ago2 as a miRNA carrier could account for all circulating miRNAs not encapsulated in vesicles. However, other miRNA complexes may also exist in plasma and remain to be discovered. The reagents currently available did not allow for a definitive analysis of the other three Ago proteins encoded by the human genome, and these additional Ago proteins may also serve as carriers of circulating miRNA. In addition, cultured fibroblasts secrete nucleophosmin 1, which is able to protect miRNA from degradation in vitro (29). It remains to be seen whether nucleophosmin 1 is present in the cell-free circulation and binds to miRNAs in vivo.

Our results strongly support the hypothesis that circulating Ago2 complexes serve as a significant carrier of miRNAs in plasma. In addition to the utility of circulating miRNAs as biomarkers of disease, the potential function of extracellular miRNAs has been an area of active investigation. Extracellular miRNAs have been proposed as a means of intercellular communication (6, 14, 16), and exosome-mediated transfer of miRNA between cells has been reported in cell culture (15) and from plasma-derived microvesicles to endothelial cells in the experimental setting (17). There is also a precedent for a protein carrier-based RNA communication mechanism in plants, in which PSRP1 is secreted into the phloem and mediates systemic cell-to-cell trafficking of small RNAs (30). Our finding of Ago2–miRNA complexes in the circulation raises the interesting possibility that, as the core catalytic component of the miRNA-induced silencing complex (22), these complexes may be poised to regulate gene expression in recipient cells.

Materials and Methods

Plasma and Serum Samples. Human plasma and serum samples from healthy donors were obtained after written informed consent was obtained, in accordance with the Declaration of Helsinki guidelines, and with ethical approval from the local institutional review boards.

Vesicle Preparation and Visualization. Vesicles were prepared by ultracentrifugation of fresh platelet-poor plasma at 120,000 × *g* for 70 min at 4 °C. Vesicles were fixed, contrasted with uranyl oxalate, and visualized by transmission EM.

Size-Exclusion Chromatography. A Sephacryl S-500 column (GE Healthcare) was injected with 0.5 mL of platelet-poor plasma or serum and eluted with PBS solution (pH 7.4) at room temperature. Fractions were stored at 4 °C before use.

RNA Isolation, qRT-PCR, and miRNA Profiling. RNA was isolated using the miRNeasy kit (Qiagen). Modifications to the manufacturer's protocol are provided in *SI Materials and Methods*. Individual miRNAs were detected by TaqMan qRT-PCR assays as described (25). Samples were profiled for 375 miRNAs by using miRNA Ready-to-Use PCR, Human Panel I, V2.M qRT-PCR arrays (Exiqon).

Immunoprecipitation and Immunoblotting. Mouse monoclonal anti-Ago2 (ab57113; Abcam) or mouse normal IgG (Santa Cruz Biotechnology) antibodies were preincubated with Magna Bind goat anti-mouse IgG Magnetic Bead slurry (Thermo Scientific) and used for immunoprecipitation of plasma and plasma fractions. Rabbit polyclonal anti-Ago2 antibody (ab32381; Abcam) was used for immunoblotting.

Details of sample processing, experimental procedures, and data analysis are provided in *SI Materials and Methods*.

ACKNOWLEDGMENTS. We thank the Fred Hutchinson Cancer Research Center EM Shared Resource for assistance in preparing samples. We also thank R. Parkin for advice and assistance with blood processing, E. Knouf and D. Kuppers for advice and helpful discussion, and A. Geballe and B. Knudsen for critical reading of the manuscript. This work was supported by an American Cancer Society Postdoctoral Fellowship (to J.D.A.), a Canary Foundation/American Cancer Society Postdoctoral Fellowship for the Early Detection of Cancer (to J.R.C.), a National Institutes of Health DK-085714 Transformative R01 grant (to M.T.), and a Damon Runyon–Rachleff Innovation Award (to M.T.).

1. Mitchell PS, et al. (2008) Circulating microRNAs as stable blood-based markers for cancer detection. *Proc Natl Acad Sci USA* 105:10513–10518.
2. Chen X, et al. (2008) Characterization of microRNAs in serum: A novel class of biomarkers for diagnosis of cancer and other diseases. *Cell Res* 18:997–1006.
3. Chim SS, et al. (2008) Detection and characterization of placental microRNAs in maternal plasma. *Clin Chem* 54:482–490.
4. Gilad S, et al. (2008) Serum microRNAs are promising novel biomarkers. *PLoS ONE* 3: e3148.
5. Lawrie CH, et al. (2008) Detection of elevated levels of tumour-associated microRNAs in serum of patients with diffuse large B-cell lymphoma. *Br J Haematol* 141:672–675.
6. Skog J, et al. (2008) Glioblastoma microvesicles transport RNA and proteins that promote tumour growth and provide diagnostic biomarkers. *Nat Cell Biol* 10: 1470–1476.
7. Taylor DD, Gercel-Taylor C (2008) MicroRNA signatures of tumor-derived exosomes as diagnostic biomarkers of ovarian cancer. *Gynecol Oncol* 110:13–21.
8. Ng EK, et al. (2009) Differential expression of microRNAs in plasma of patients with colorectal cancer: a potential marker for colorectal cancer screening. *Gut* 58: 1375–1381.
9. Ai J, et al. (2010) Circulating microRNA-1 as a potential novel biomarker for acute myocardial infarction. *Biochem Biophys Res Commun* 391:73–77.
10. Jackson DB (2009) Serum-based microRNAs: are we blinded by potential? *Proc Natl Acad Sci USA* 106:E5.
11. Février B, Raposo G (2004) Exosomes: Endosomal-derived vesicles shipping extracellular messages. *Curr Opin Cell Biol* 16:415–421.
12. Heijnen HF, Schiel AE, Fijnheer R, Geuze HJ, Sixma JJ (1999) Activated platelets release two types of membrane vesicles: Microvesicles by surface shedding and exosomes derived from exocytosis of multivesicular bodies and alpha-granules. *Blood* 94:3791–3799.
13. Hunter MP, et al. (2008) Detection of microRNA expression in human peripheral blood microvesicles. *PLoS ONE* 3:e3694.
14. Valadi H, et al. (2007) Exosome-mediated transfer of mRNAs and microRNAs is a novel mechanism of genetic exchange between cells. *Nat Cell Biol* 9:654–659.
15. Kosaka N, et al. (2010) Secretory mechanisms and intercellular transfer of microRNAs in living cells. *J Biol Chem* 285:17442–17452.
16. Pigati L, et al. (2010) Selective release of microRNA species from normal and malignant mammary epithelial cells. *PLoS ONE* 5:e13515.
17. Zhang Y, et al. (2010) Secreted monocytic miR-150 enhances targeted endothelial cell migration. *Mol Cell* 39:133–144.
18. Rabinowits G, Gerçel-Taylor C, Day JM, Taylor DD, Kloecker GH (2009) Exosomal microRNA: a diagnostic marker for lung cancer. *Clin Lung Cancer* 10:42–46.
19. Song JJ, et al. (2003) The crystal structure of the Argonaute2 PAZ domain reveals an RNA binding motif in RNAi effector complexes. *Nat Struct Biol* 10:1026–1032.
20. Ma JB, Ye K, Patel DJ (2004) Structural basis for overhang-specific small interfering RNA recognition by the PAZ domain. *Nature* 429:318–322.
21. Meister G, et al. (2004) Human Argonaute2 mediates RNA cleavage targeted by miRNAs and siRNAs. *Mol Cell* 15:185–197.
22. Valencia-Sanchez MA, Liu J, Hannon GJ, Parker R (2006) Control of translation and mRNA degradation by miRNAs and siRNAs. *Genes Dev* 20:515–524.
23. McPherson R, Pincus M, eds (2007) *Henry's Clinical Diagnosis and Management by Laboratory Methods* (Saunders Elsevier, Philadelphia), 21st Ed.
24. Heneghan HM, et al. (2010) Circulating microRNAs as novel minimally invasive biomarkers for breast cancer. *Ann Surg* 251:499–505.
25. Kroh EM, Parkin RK, Mitchell PS, Tewari M (2010) Analysis of circulating microRNA biomarkers in plasma and serum using quantitative reverse transcription-PCR (qRT-PCR). *Methods* 50:298–301.
26. Kim VN, Han J, Siomi MC (2009) Biogenesis of small RNAs in animals. *Nat Rev Mol Cell Biol* 10:126–139.
27. Chang J, et al. (2004) miR-122, a mammalian liver-specific microRNA, is processed from hcr mRNA and may downregulate the high affinity cationic amino acid transporter CAT-1. *RNA Biol* 1:106–113.
28. Blanc L, Vidal M (2010) Reticulocyte membrane remodeling: Contribution of the exosome pathway. *Curr Opin Hematol* 17:177–183.
29. Wang K, Zhang S, Weber J, Baxter D, Galas DJ (2010) Export of microRNAs and microRNA-protective protein by mammalian cells. *Nucleic Acids Res* 38:7248–7259.
30. Yoo BC, et al. (2004) A systemic small RNA signaling system in plants. *Plant Cell* 16: 1979–2000.